

**ECONOMIC GEOLOGY
RESEARCH UNIT**

University of the Witwatersrand
Johannesburg

— . —

A PRELIMINARY INVESTIGATION OF
FLUID-INCLUSIONS IN THE
PILGRIM'S REST GOLDFIELD, EASTERN TRANSVAAL

J.P. ASH and N. TYLER

UNIVERSITY OF THE WITWATERSRAND
JOHANNESBURG

A PRELIMINARY INVESTIGATION OF FLUID-INCLUSIONS IN
THE PILGRIM'S REST GOLDFIELD, EASTERN TRANSVAAL

by

J. P. ASH and N. TYLER

*(Department of Geological Sciences,
University of Texas, Austin, Texas, U.S.A.)
(Bureau of Economic Geology
University of Texas, Austin, Texas, U.S.A.)*

ECONOMIC GEOLOGY RESEARCH UNIT
INFORMATION CIRCULAR No. 180

February, 1986

A PRELIMINARY INVESTIGATION OF FLUID-INCLUSIONS IN
THE PILGRIM'S REST GOLDFIELD, EASTERN TRANSVAAL

ABSTRACT

The Pilgrim's Rest Goldfield encompasses a cluster of quartz-pyrite-gold veins that outcrop and subcrop over an area of 600 sq. km. in the eastern Transvaal. Most of the veins are found in the Malmani Dolomite of the 2200-m.y.-old Transvaal Supergroup; lesser numbers of veins crosscut the granitic basement or follow bedding in the Wolkberg and Pretoria Groups that underlie, and rest on, the Malmani Dolomite, respectively.

Six samples of vein-quartz, two from vertical veins in the basement granite, two from strata-bound, bedded ore-bodies ("reefs") in the dolomite, and two from stockworks that accompany the bedded reefs, were selected for fluid-inclusion analysis. Pilgrim's Rest fluid-inclusions are highly complex. Four principal types have been recognized. Type-1 inclusions are entirely aqueous; Type-2 contain mixtures of $\text{CO}_2 \pm \text{H}_2\text{O} \pm \text{CH}_4$; Type-3 are characterized by the presence of variable quantities of daughter-minerals halite, sylvite, and anhydrite, in addition to liquid- and vapor-phases; Type-4 inclusions are nearly-pure CO_2 . The fluid-inclusions are variable in density and composition. Inclusions containing high-density, CO_2 -rich fluids are ubiquitous. Aqueous inclusions exhibit moderate-to-high salinities.

Temperature-determinations indicate that the inclusions were trapped under a temperature gradient of $100^\circ\text{C}/\text{km}$. Inclusions from quartz veins cutting basement granites homogenize at between 300° and 400°C ; inclusions from shallower, strata-bound reefs homogenize at 200°C . Each sample displays a range of homogenization- and decrepitation-temperatures, suggesting that mineralization was probably a multiphase event. Preliminary geobarometry suggests depths-of-formation of 5,5-7,0 km. Pilgrim's Rest fluid-inclusions are similar, in many respects, to those in Archean lode-gold deposits.

A PRELIMINARY INVESTIGATION OF FLUID-INCLUSIONS IN
THE PILGRIM'S REST GOLDFIELD, EASTERN TRANSVAAL

CONTENTS

	<u>Page</u>
<u>INTRODUCTION</u>	1
<u>ANALYTICAL PROCEDURES</u>	2
<u>RESULTS</u>	4
Theta Reef	4
Blyde Reef	6
Vaalhoek Stockwork	8
Trixie Leader	8
Gregory Reef	9
Rietfontein Reef	10
<u>IMPLICATIONS FOR THE ORIGIN OF THE PILGRIM'S REST VEIN-DEPOSITS</u>	11
<u>CONCLUSIONS</u>	17
REFERENCES	18

————— oOo —————

Publication Authorized by the Director,
Bureau of Economic Geology, University of Texas at Austin

*

Published by the Economic Geology Research Unit
University of the Witwatersrand
1 Jan Smuts Avenue
Johannesburg 2001

ISBN 0 85494 916 X

A PRELIMINARY INVESTIGATION OF FLUID-INCLUSIONS IN
THE PILGRIM'S REST GOLDFIELD, EASTERN TRANSVAAL

INTRODUCTION

The Pilgrim's Rest Goldfield consists of a cluster of discrete, quartz-pyrite-precious-metal veins that outcrop and subcrop over an area of 600 sq. km. centred on the historic village of Pilgrim's Rest in the eastern Transvaal. The deposits have been exploited continuously for over a hundred years, during which time 155 metric tonnes (5 million ounces) of gold and an unknown, but probably comparable, amount of silver have been produced. Initially, exploration focused on modern, placer deposits, but these were soon worked out and attention shifted, in the late-1870's, to exploration for, and exploitation of, the accompanying strata-bound ore-bodies. The principal ore-bodies lie mainly in the Malmani Dolomite of the Transvaal Supergroup; however, mineralized vein-systems also crosscut the granitoid basement and occur as bedded, tabular deposits in the proto-basinal phase of the Transvaal Supergroup (Wolkberg Group), in the Black Reef Quartzite, and in the basal members of the Pretoria Group.

The ore-bodies display well-defined, areal and stratigraphic distributions. Areally, they occur in three groups : around Sabie, around Pilgrim's Rest, and between Vaalhoek and Bourke's Luck. Intervening areas have proved devoid of significant mineralization. Stratigraphically, the ores are localized in three zones : (1) in clastic sediments in the Wolkberg Group and the Black Reef Quartzite and in the overlying clastic-carbonate transition of the Malmani Dolomite; (2) in the lower dolomite-and-chert zone of the Malmani Dolomite; (3) and in the upper dolomite-and-chert zone of the Malmani Dolomite and in basal units of the Pretoria Group.

The 2200-m.y.-old Transvaal Supergroup, which hosts almost all of the mineralization at Pilgrim's Rest, was deposited on a stable craton. Fluvial sediments filled paleovalleys on the granite-greenstone basement and gave way, with time (and vertically), to shallow-marine deposition. Volcanism periodically interrupted sedimentation. By Black Reef time, the paleotopography on the basement had been filled, and an extensive epicontinental sea covered the craton. As erosion took its toll on the provenance, clastic sediments became finer-grained, increasingly argillaceous, and less abundant, so that, by early-Malmani time, the sea was largely clear of clastic sediment, except for minor storm-events and local, minor, deltaic depo-centers. Carbonate sedimentation during Malmani time took place on a broad, restricted platform; the resulting, algal sediments display mostly shallow-subtidal-to-intertidal characteristics, with the exception of a major transgression, during which time deep-water, shelf-edge sediment (the chert-poor zone) was deposited. The depositional history of the host-rocks plays a significant role in the emplacement history of the tabular ore-bodies. The ores are clearly localized in sediments of shallow-subtidal-to-intertidal origin. Deeper-water, shelf sediments are barren.

Precious-metal veins at Pilgrim's Rest display two, fundamental morphologies. Most of the gold and silver has been derived from strata-bound, tabular ore-bodies (also known as lodes or reefs) that are largely conformable with bedding, but may be locally transgressive. They are laterally-extensive, sheetlike, regularly-bedded units that "calcite-out"

(i.e., become increasingly calcareous) away from the area of highest gold values. The other, major category consists of vertical, quartz veins which are frequently associated with shear-zones, dykes, and faults and which commonly trend northward. One of these vertical bodies (the Rietfontein Reef), which has been extensively mined, displays great vertical and lateral extent. Accompanying these two, principal categories of ore-bodies are stockworks, "leaders" (thin transgressive veins associated with the strata-bound, tabular ore-bodies), "blows" (elongate, thickened bodies, also related to the flat reefs), and a variety of smaller, irregular ore-bodies. Mineralogically, they are all similar and consist of quartz, pyrite, and carbonate gangue and minor, pyritized, wall-rock fragments. The more-important ore-minerals are arsenopyrite, chalcopyrite, tetrahedrite, bismuthinite, and bismuth. Locally, minor amounts of galena, pyrrhotite, bornite, sphalerite, scheelite, and visible gold are also present (Swiegers, 1948).

This paper presents the results of a study of fluid-inclusions in quartz gangue from gold-bearing veins in the Pilgrim's Rest Goldfield. Six, quartz-vein samples were studied, using petrographic and micro-thermometric techniques, outlined by Roedder (1984), to estimate the pressure-temperature ranges present during quartz-precipitation and to define the composition(s) of the ore-fluids trapped under those P-T conditions.

Samples of vein-quartz were selected from six ore-bodies. Two samples were from vertical lodes (Sample 6R5B-326 from the Rietfontein Reef and Sample 92 from the Gregory Reef, both of which cut across basement granites). Two samples were obtained from tabular, strata-bound ore-bodies (Sample BRI-022 from the Blyde Reef, at the top of the lower dolomite-and-chert zone and Sample DHC-5 from the Theta Reef, in the upper dolomite-and-chert zone). The remaining two samples were taken from irregular bodies. Sample BFT-1A was obtained from the Trixie Leader, in the Wolkberg Group, and Sample FT1-3 from a stockwork associated with the Vaalhoek Reef, in the lower dolomite-and-chert zone. The samples were purposely selected to provide information on as wide a range of ore-body types as possible and on ore-bodies found at differing levels in the stratigraphic section. Fluid-inclusion sample-preparation procedures followed in this study have been fully described by Roedder (1984).

ANALYTICAL PROCEDURES

The fluid-inclusions were examined with a Leitz Ortholux microscope, equipped with a fluid-inclusion-adapted, U.S.G.S., gas-flow, heating/freezing system, in the Department of Geological Sciences, University of Texas at Austin. Temperatures from -180°C to +700°C are readily obtained, using circulating, refrigerated, nitrogen-gas and an electric-torch heating-element. The approximate compositions of the fluids were determined by the direct observation of phase-changes in individual inclusions and by comparing observed temperatures with experimentally-determined equilibria (Collins, 1979; Hollister and Burruss, 1976).

The samples consisted of doubly-polished, 0,2-0,4 mm-thick wafers of quartz and gangue-minerals. These "thick sections" were initially studied

and photographed, prior to removal from the glass-slide. Rough estimates of the relative abundance of different types of inclusions were made by visually estimating the percentage in the field-of-view of the microscope, using percentage charts and taking the average of 10 fields. Areas chosen for detailed study were then broken into 0,5-1-cm² fragments for micro-thermometric study. Fragments were secured in the heating/freezing chamber by an Omega wire-thermocouple.

Maximum magnification and resolution of the optical image were obtained with a Leitz H32 long-range-focus objective and 16x oculars. Examination of large (>20 micron) inclusions was enhanced by using a 10x objective with greater-resolution characteristics. Factors such as intensity of light-source, filters, condenser-position, and diaphragm-apertures were adjusted to maximize resolution of the image. These factors were held constant throughout the study, to ensure consistent temperature-measurements.

Due to the abundance of CO₂ in the Pilgrim's Rest samples, as determined from petrographic surveying, crushing tests were conducted on broken fragments of the original samples, as described by Roedder (1984). These tests confirmed the presence of a dense CO₂-phase in all of the samples. As a result of these initial findings, freezing-point determinations were conducted before homogenization-tests, to prevent decrepitation in the samples. Samples were rapidly cooled to -120°C, at a rate of 30°C/min, reheated to -75°C, and then slowly heated to T_m(CO₂) - the melting temperature of solid CO₂ - at a rate of 0,2-0,5°C/min. Rapid heating to approximately -30°C was followed by slower rates of heating, until T_m(ice) and/or T_m(clathrate) were determined.

The heating/freezing stage was calibrated with the following, pure, substances, sealed in capillary tubes. A flow-rate of 40 SCFH was used in all calibration-runs.

<u>Substance</u>	<u>Melting Point (°C)</u>	<u>Measured Temperature (°C)</u>
Tin	231,9	230,1
Bismuth	271,3	273,4
Zinc	419,6	416,7
Antimony	630,7	625,8

<u>Substance</u>	<u>Melting Point (°C)</u>	<u>Measured Temperature (°C)</u>
Water	0,01	0,0
n-Dodecane	-9,6	-9,6
o-Xylene	-25,2	-25,4
CO ₂	-56,6	-56,7

Between -60°C and +100°C, results were reproducible to +0,2°C and no corrections were applied to the data. The system was regularly recalibrated, using a distilled-water ice-bath.

RESULTS

The quartz-vein samples consisted predominantly of quartz, pyrite (locally weathered to Fe-oxides), subordinate dolomite, and pyritized, carbonaceous, shale gangue. The petrographic fabric of the quartz in the samples varied from coarsely-crystalline, euhedral quartz (Theta Reef, Trixie Leader) to massive, bull quartz (Blyde Reef, Gregory Reef). One sample (Rietfontein Reef) contained recrystallized, cloudy quartz, cut by conjugate microfractures healed with limonite. Deformation in this sample confirmed the longevity of movement in the Rietfontein Shear, with which this reef is associated. However, with the exception of occasional, sutured, quartz-grain boundaries, the other Pilgrim's Rest samples show no evidence of significant metamorphism or recrystallization.

The Pilgrim's Rest samples contain abundant fluid-inclusions that are variable in density and composition, ranging from nearly-pure CO_2 (Type 4) (Fig. 1), through $\text{CO}_2+\text{H}_2\text{O}+\text{CH}_4$ -mixtures, to inclusions which are entirely aqueous (Types 1 and 2) (Fig. 1). The inclusions can contain one or more of the following phases : $\text{CO}_2(\text{L})$, $\text{CO}_2(\text{L}+\text{V})$, $\text{H}_2\text{O}(\text{L})$, $\text{H}_2\text{O}(\text{L}+\text{V})$, an halite daughter-mineral, a sylvite daughter-mineral, an anhydrite daughter-mineral, and an unknown daughter-mineral. Inclusions containing an halite daughter-mineral, with or without associated daughter-minerals, are classified as Type-3 inclusions (Fig. 1). The presence of trace-amounts of CH_4 is suggested in some inclusions containing a dense ($>0,85 \text{ g/cm}^3$) CO_2 -phase. The density and fluid-composition data were obtained from direct observations of phase-changes between -120°C and $+450^\circ\text{C}$ and by comparing these data with published experimental data in the appropriate multi-component system.

The following section describes fluid-inclusion characteristics of the six samples of Pilgrim's Rest vein-quartz. The results of the micro-thermometric analysis are tabulated in Appendix 1.

Theta Reef

Sample DHC-5 is composed of coarsely-crystalline, subhedral-to-euhedral, milky-white quartz, with pyritized carbonaceous-shale bands. Quartz is cloudy, due to the presence of dense patches of fluid-inclusions throughout the sample. Clear, isolated areas ($1 \times 2 \text{ mm}$) in the interior portions of the quartz crystals contain lower concentrations of larger (10-50 micron) inclusions. The greater concentration of inclusions ($<10 \text{ microns}$) at grain-boundaries and the presence of secondary inclusion-planes crossing grain-boundaries suggest that some post-quartz deformation occurred in Sample DHC-5. Irregularly-distributed, opaque "inclusions" in these areas may represent fluid-inclusions that decrepitated prior to petrographic examination. The carbonaceous shale is finely laminated. Coarse-grained (5 mm), euhedral, pyrite cubes comprise 10-15% of the shaly material, although subordinate amounts of pyrite are present in the quartz.

The Theta Reef is characterized by abundant, large ($>25 \text{ micron}$), CO_2 -rich inclusions which comprise more than 48 per cent of the inclusions in the sample. The CO_2 -phase is generally very dense ($>0,85 \text{ g/cm}^3$) and estimates of mole-per cent CO_2 yield a range of 25-60 per cent. Melting-point-depression measurements indicate the CO_2 -phase is essentially-pure

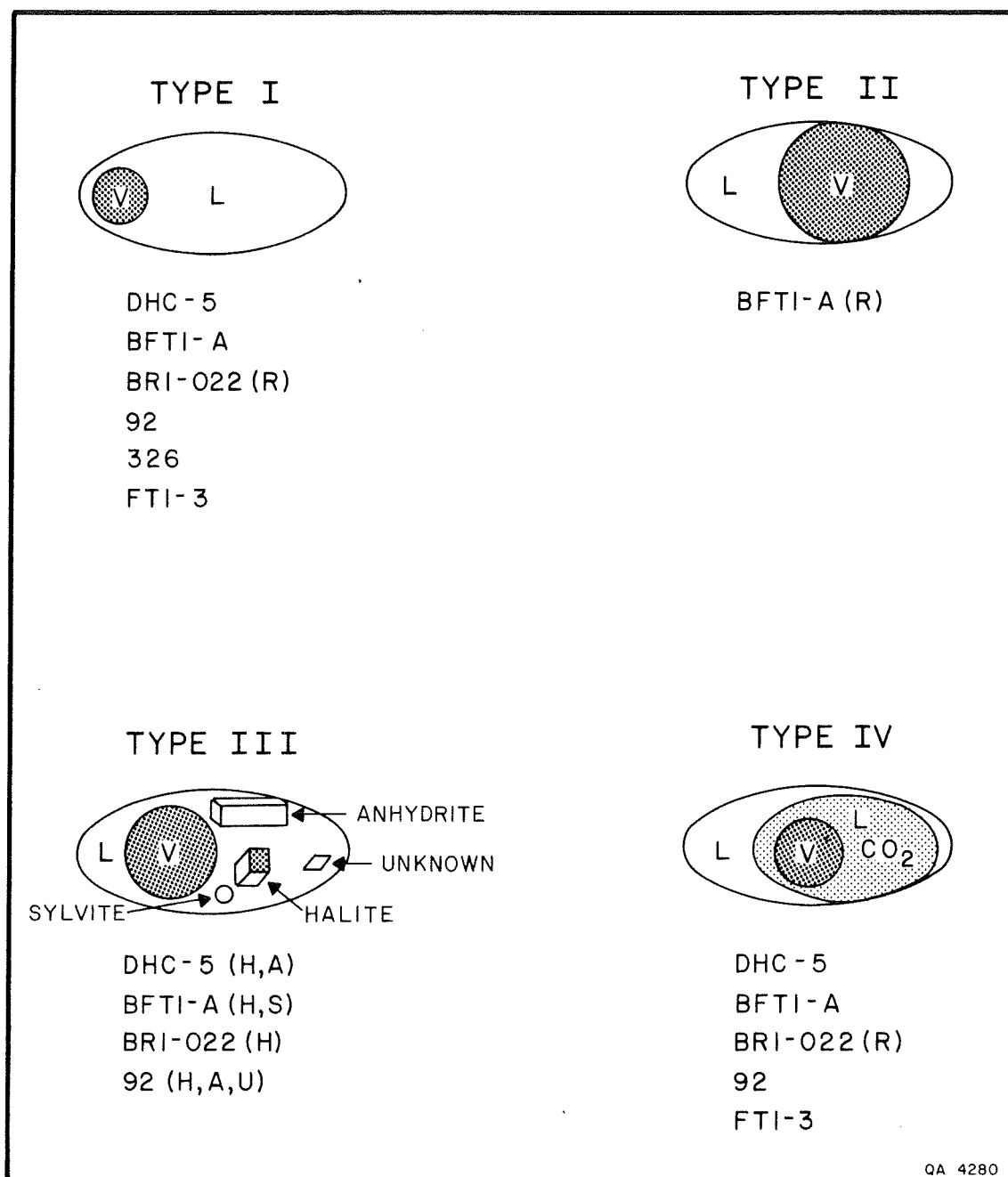


Figure 1 : Schematic illustration of fluid-inclusion types observed in the Pilgrim's Rest veins. Samples containing various types of inclusions are listed. (R) occurs in trace amounts; (H) halite daughter-mineral; (A) anhydrite; (S) sylvite; (U) unknown daughter-mineral. After Nash (1972).

CO₂; however, in inclusions with greater than 75 volume-per cent CO₂, the presence of trace-amounts of other solutes (i.e. CH₄) is suggested by T_m (CO₂) less than -56,6°C. Crushing tests also suggest the presence of CH₄.

The remaining inclusions in Sample DHC-5 consist of : $\text{H}_2\text{O}(\text{L}+\text{V})$; $\text{H}_2\text{O}(\text{L}+\text{V}) + \text{halite} \pm \text{anhydrite}$; and $\text{H}_2\text{O}(\text{L}+\text{V}) + \text{CO}_2(\text{L}) \pm \text{halite}$ (Fig. 1). Aqueous inclusions and/or CO_2 -poor inclusions are preferentially located along secondary planes that often cross quartz-grain boundaries. Homogenization-temperatures for CO_2 - H_2O and H_2O - NaCl inclusions range from 185°C to 325°C. Decrepitation of CO_2 -rich inclusions was common above 200°C (Fig. 2).

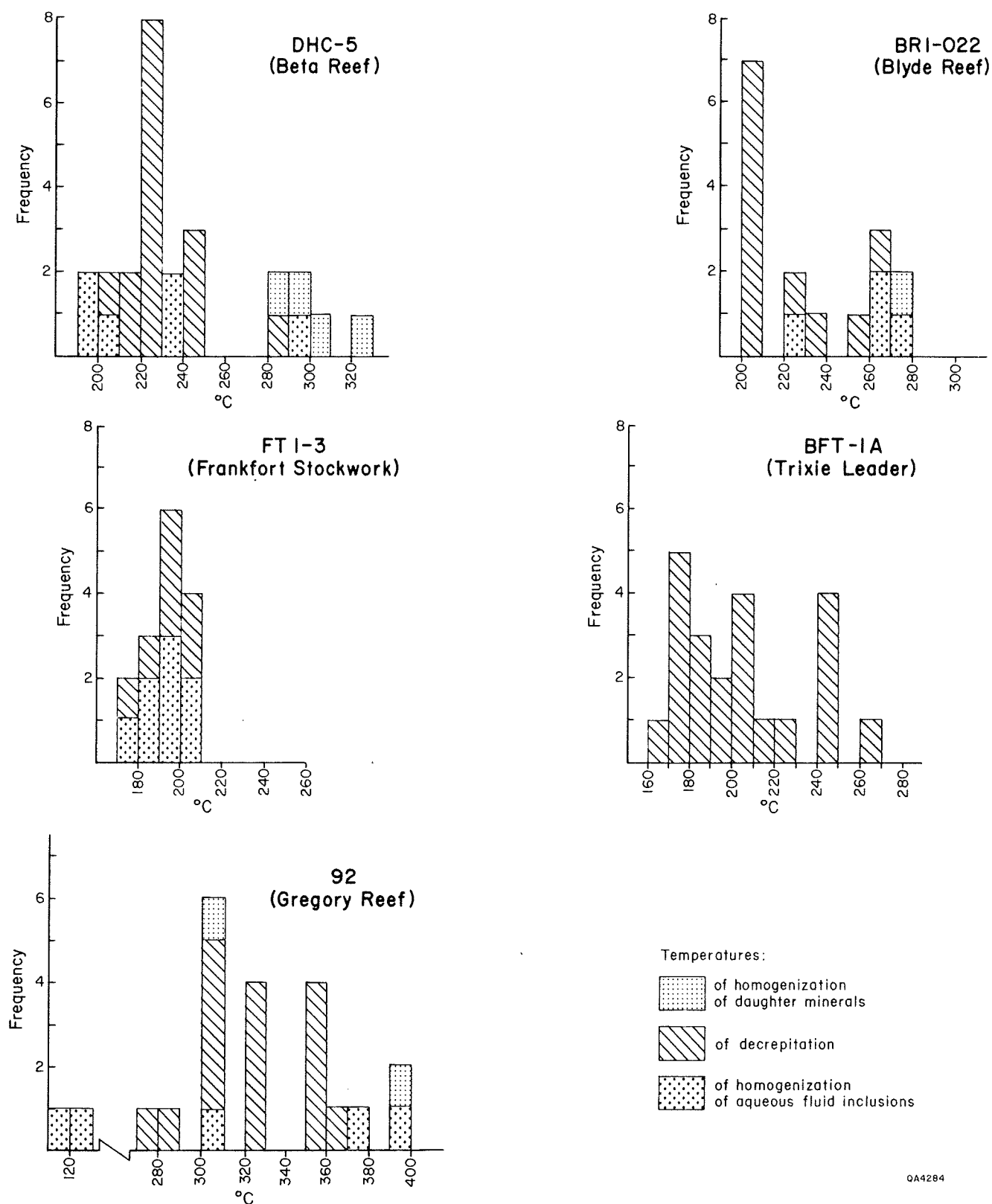
Halite and a birefringent daughter-crystal, tentatively identified as anhydrite, are the only solid inclusions observed in Sample DHC-5. Halite occurs in less than 5% of the inclusions, is present in consistent phase-ratios, and is always the last phase present before total homogenization or decrepitation. The anhydrite daughter-phase is present in only a few inclusions and may represent "accidental inclusions" (Roedder, 1984). Homogenization of this daughter-mineral to the liquid phase was not observed in Sample DHC-5.

The presence of CO_2 and the possible presence of divalent cations, such as Ca^{++} (as suggested by the anhydrite daughters), complicate the interpretation of the salinity-data in this sample (Roedder, 1984). These solutes tend to decrease the solubility of NaCl , causing a halite daughter to be present, even though the solution contains less than 26,5 weight-per cent NaCl -equivalent. In simple NaCl - H_2O at STP, the presence of a halite daughter-mineral indicates the solution contains a minimum of 26,5 weight-per cent NaCl -equivalent. The presence of halite indicates the trapped fluid is oversaturated with respect to NaCl at laboratory conditions. However, freezing-point-depression measurements on aqueous and/or CO_2 -poor inclusions in Sample DHC-5 suggest salinity values ranging from 9 to 17 weight-per cent NaCl -equivalent. The accuracy of this measurement is, in turn, complicated by the formation of clathrate hydrates between +2 to +14°C, which tends to increase the salinity of the residual, aqueous fluid. No effort to evaluate the relative influences of these opposing effects has been made in this study.

Blyde Reef

Sample BR1-022 consists of massive, milky-white quartz, with deformed laminae of unoxidized, pyritic, black shale. The quartz contains abundant fractures, some of which are healed with pyrite. Pyrite occurs preferentially in the shale as thin (1 mm), continuous bands and as euhedral cubes (1-5 mm), near contacts with the quartz. X-ray-diffraction analysis indicates the presence of trace-amounts of chalcopyrite in the shaly material.

With the exception of the Vaalhoek stockwork (FT1-3), this sample from the Blyde Reef exhibited the largest range in CO_2 -content of the Pilgrim's Rest samples. The estimated densities and molar-percentages of CO_2 -phases are 0,87-0,92 g/cm³ and 10 to more than 60 mole-per cent CO_2 , respectively. The presence of additional, lower-density inclusions in this sample is indicated by slightly-higher $T_h(\text{CO}_2)$ of up to + 18°C. Regardless of the volume of the inclusion occupied by the CO_2 -phase, freezing-point-depression measurements indicate a relatively-pure CO_2 -phase. No total homogenization-temperatures above 275°C were recorded in these inclusions, due to widespread decrepitation at around 200°C (Fig. 2). The high density



QA4284

Figure 2 : Histogram-plots of temperatures-of-homogenization of aqueous inclusions, temperatures-of-homogenization of daughter-minerals, and temperatures-of-decrepitation of CO₂-rich inclusions.

of the CO₂-phase in BR1-022 is the likely cause of the relatively-low temperature-of-decrepitation.

Halite daughter-minerals occur in less than 1% of the inclusions and occupy between 5 and 10 volume-per cent of those inclusions. No other daughter-minerals were observed in this sample. Aqueous fluid-inclusions in BR1-022 are rare and generally too small (<10 microns) for salinity-determinations.

Vaalhoek Stockwork

Sample FT1-3 consists of euhedral, cloudy, quartz crystals and coarsely-crystalline and massive dolomite, with subordinate pyrite. The quartz is coarse-grained, generally euhedral, and clouded with abundant fluid-inclusions. Euhedral, quartz overgrowths on pyrite and isolated, 2-5 mm, quartz crystals, with hexagonal cross-sections, are spatially associated with the massive, dolomite phases in the sample and may represent a later period of quartz-precipitation. Insufficient data were collected to confirm this hypothesis. Pyrite is euhedral and forms perfect cubes, especially when associated with dolomite. Intergrown, pyrite grains are similarly well-formed, suggesting slow precipitation, without significant transport.

The fluid-inclusions in this sample are characterized by the absence of associated, daughter-mineral phases and relatively wide ranges in volume-per cent CO₂ (<5,85%) in coexisting fluid-inclusions. The densities of this phase are comparable to, but slightly higher than, those observed in other CO₂-rich samples, ranging from 0,65 to 0,93 g/cm³. The majority of the CO₂-rich inclusions exhibit (T_h(CO₂)) of +1 to +6°C, corresponding to a density range of 0,88-0,92 g/cm³.

Homogenization-temperatures are grouped around 190°-200°C, with decrepitation also common at, or above, these temperatures (Fig. 2). Salinity-measurements of H₂O ± CO₂ inclusions yield values that exceed 20 weight-per cent NaCl-equivalent. No daughter-minerals occur in Sample FT1-3.

Trixie Leader

Sample BFT-1A consists of coarse-grained, euhedral, vein-quartz, with black, carbonaceous-shale gangue. Pyrite (2-5 volume-per cent) and trace chalcopyrite preferentially occur with the shaly material. Pyrite is euhedral and forms cubes up to 5 mm in length. Chalcopyrite occurs as fine, irregular inclusions in the coarser, pyrite cubes. No replacement fabric was observed in this sample.

Fluid-inclusions in the Trixie Leader are characterized by an abundance of CO₂-rich inclusions, with equant shapes and pseudo-hexagonal symmetry. Obvious, secondary inclusions tend to be much smaller and are simple liquid-vapour in composition (L>>V) and lack a recognizable CO₂-phase. The densities and mole-per cent CO₂ in this sample are generally lower (0,65-,80 g/cm³ and 0-30 per cent, respectively) than in the other CO₂-rich samples. When CO₂(L) occupies less than 20 volume-per cent of an inclusion, an active CO₂(V)-phase is present at laboratory temperature and pressure.

Halite daughter-minerals occur in less than 1% of all inclusions and are more common in aqueous and/or CO₂-poor inclusions. Freezing-point-depression measurements in aqueous inclusions suggests BFT-1A inclusions contain less saline fluids, with estimated salinities ranging from 2 to 12 weight-per cent NaCl-equivalent. However, the occurrence of a small, circular, isotropic daughter-mineral (tentatively identified as sylvite) complicates the interpretation of the salinity-data. The presence of other dissolved solutes, such as sylvite, tends to lower the solubility of halite, thus causing formation of an halite daughter-mineral in lower-NaCl-equivalent solutions.

Homogenization-temperatures are unclear in Sample BFT-1A. CO₂-rich inclusions tend to decrepitate above 175-225°C (Fig. 2), and aqueous inclusions often fail to homogenize, even at temperatures exceeding 400°C. Total decrepitation of the sample occurred above 300°C.

Gregory Reef

Sample 92 consists of a 20 cm-long slab of borehole-core across sulphide-rich and sulphide-poor zones in massive-to-anhedraal vein-quartz. The sulphide-rich portion is vuggy, and all sulphides have been oxidized to a mixture of limonites. The vugs comprise about 30 volume-per cent of the sulphide-rich quartz and occur as irregularly-shaped voids, coated with limonites and finely-crystalline, "drusy" quartz. This "drusy" quartz is post-oxidation and is considered to be a supergene product, unrelated to hydrothermal, gold mineralization. Sulphide-poor quartz is similar in morphology and texture to the sulphide-rich quartz, with the exception of the vuggy nature of the sulphide-rich portion.

Fluid-inclusions in the Gregory Reef are characterized by an abundance of daughter-minerals. Daughter-minerals occur in 10-15% of the inclusions, and there is frequently more than one daughter-mineral present in 30% of the inclusions with daughter-minerals. Daughter-minerals preferentially occur in aqueous and/or CO₂-poor inclusions. Some daughter-crystals did not homogenize, even at temperatures as high as 450°C. Some of these could be "accidental", solid inclusions, as suggested by Roedder (1984). However, the regularity of phase-ratios and the fact that the majority of daughter-minerals do homogenize to the liquid phase support the interpretation that the majority of the daughter-crystals are true daughter-minerals.

Halite was identified as the predominant daughter-mineral phase and was always present if another daughter-mineral were present. Halite occupies 5-10 volume-per cent of the inclusions and is isotropic under crossed nicols. Anhydrite is tentatively identified as the next-most-common daughter-mineral, on the basis of petrographic criteria. This phase is rectangular and birefringent, has parallel extinction and moderate relief, and is length-slow in the position of minimum birefringence. Daughter-minerals always melt after the disappearance of the vapour-phase, usually above temperatures of 225°C-300°C. Another, highly-birefringent daughter-mineral of rhombic habit, that occurs as solid inclusions within the quartz crystals, as well as within the fluid-inclusions, has been tentatively identified as a carbonate.

Salinity-measurements for CO₂-rich inclusions yield values that exceed 23 weight-per cent NaCl-equivalent. The presence of abundant, halite daughter-minerals and other, less-prevalent daughter-minerals, such as anhydrite, suggests that the Gregory Reef fluid-inclusions contain the highest concentration of total dissolved solids of all the Pilgrim's Rest samples studied. Salinity-measurements for aqueous inclusions yield values of 12-25 weight-per cent NaCl-equivalent.

CO₂ is a much less dominant phase in this sample and less than 20 per cent of the inclusions contain an identifiable CO₂-phase. However, T_h(CO₂) indicates the inclusions contain a very dense CO₂-phase, ranging from 0,87 to 0,95 g/cm³. The estimated molar-per cent (CO₂) in Sample 92 ranges from 15 to 35 per cent. The presence of other solutes, such as CH₄ and SO₄, was not suggested during melting-point tests, except in those inclusions containing greater than 50 volume-per cent CO₂.

Homogenization-temperatures in Sample 92 are the highest of the six Pilgrim's Rest samples studied (Fig. 2). Decrepitation of the sample is common above 300-350°C, although one CO₂-H₂O inclusion homogenized at 295°C. Aqueous inclusions that persisted after widespread decrepitation consistently homogenized to the liquid phase between 335 and 375°C.

Rietfontein Reef

Sample 6F5B-326 consists of a very cloudy, massive quartz, criss-crossed by abundant limonite-healed, conjugate microfractures. Quartz veins show signs of pressure-solution and crystal-deformation (undulose extinction under cross-polars). Almost all of the inclusions are secondary. Planes of secondary fluid-inclusions (<5-10 microns in size) cross grain-boundaries and have probably destroyed any primary fluid-inclusions present in the sample prior to deformation. X-ray-diffractometer analysis of this sample lacked any traces of low-grade, metamorphic minerals, e.g. chlorite, sericite, etc.

Fluid-inclusions were too small to be of use in analyzing phase-relationships in this sample. Some, large (20 micron) inclusions were observed, but these were interpreted as secondary inclusions that "necked-down", after reaching the two-phase boundary on a P vs. T phase-diagram. Vapour-to-liquid ratios varied widely, even in adjacent fluid-inclusions. As a result, no useful micro-thermometric data were obtained from this sample.

Sample 326 is unique among the Pilgrim's Rest samples in that there is a remarkable consistency in size and distribution of inclusions. Inclusions are between 0,5 and 10 microns in the longest dimension. Also, all of the fluid-inclusions observed in this sample were liquid and vapour inclusions (volume-per cent L>>V). The presence of CO₂ is suggested by crushing tests, but could not be confirmed by petrographic or micro-thermometric data.

IMPLICATIONS FOR THE ORIGIN OF THE PILGRIM'S REST VEIN-DEPOSITS

Fluid-inclusions from a variety of ore-body types at different stratigraphic levels in the Pilgrim's Rest Goldfield display several unifying characteristics that point towards a common genesis for these diverse deposits. Carbon-dioxide-rich fluid-inclusions are typical of this suite of samples, and the CO₂-rich inclusions all display high CO₂-densities. Further, those samples, in which salinities could be determined, exhibit moderate-to-high salinities (Table 1). Homogenization- and decrepitation-temperatures suggest a temperature-of-formation gradient of between 300 and 400°C for the deeper deposits, to temperatures of around 200°C, for the shallower ore-bodies. The present study, therefore, suggests that the spectrum of ore-bodies present in the Pilgrim's Rest Goldfield is the product of vertically-migrating, CO₂-rich, metal-bearing brines that circulated through planes of weakness, such as shear-zones (Rietfontein Reef), tectonic fractures, and dyke-filled fractures (Gregory Reef). These fluids also spread laterally into accessible, permeable, clastic and carbonate beds that may or may not have been sites of bedding-plane slip, thus forming the strata-bound, tabular ore-bodies characteristic of the Pilgrim's Rest Goldfield.

The range of T_h of the majority of the CO₂-rich phases in the samples (T_hCO₂ = -2 to 28°C) suggests entrapment over a range of temperatures and pressures. Figure 3 shows the temperature-of-homogenization of CO₂ in CO₂-rich inclusions. Individual samples, however, display a tight clustering of median temperatures-of-homogenization, that occur over a 6°-range or less. Synthesis of T_h(CO₂) of pure-CO₂ inclusions with homogenization- and decrepitation-temperatures facilitates an estimation of the pressures-of-formation of the fluid-inclusions and, by inference, the pressures-of-formation of the quartz veins (Fig. 4). Assuming average temperatures-of-formation of between 200 and 400°C, formation under lithostatic pressures, and utilizing the CO₂-isochore data of Hollister and Burruss (1976), as illustrated on Figure 4, the total possible range of pressures-of-formation is 0,5-3,2 kbar. Because of the inherent difficulties in estimating homogenization-temperatures, more confidence is felt utilizing median, rather than maximum, homogenization-values to estimate pressures-of-formation. It is realized, however, that the pressure-values obtained represent minimum values and that formation-pressures could be considerably greater.

Median homogenization-temperatures used in the calculation are tabulated in Figure 4. Based on these parameters, entrapment-pressures of the strata-bound ore-bodies are estimated to be approximately 1,4-1,5 kbars; entrapment-pressure of the Gregory Reef is 1,9 kbars (Fig. 4). These pressures translate to depths-of-entrapment of 5,5 km, for the upper, strata-bound ore-bodies and 7 km for the vertical reefs, respectively. The difference (1 500 m) in the calculated depths-of-formation for the strata-bound and vertical ore-deposits corresponds approximately to the stratigraphic interval separating the deposits (1 000 m).

The leader and stockwork pressure-data are inconsistent with that of the strata-bound and vertical reefs. Decrepitation-temperatures of the Trixie Leader suggest an anomalously-low formation-pressure of 0,8 kbars. Some of the aqueous fluid-inclusions in this sample had not homogenized, even at 400°C. Using this T_h (max) of 400°C, formation-pressure is 1,6 kbars.

**TABLE 1. SUMMARY OF PHYSICAL AND CHEMICAL CHARACTERISTICS
OF PILGRIMS REST FLUID INCLUSIONS**

Deposit	T _h (°C)	T _{decrep} (°C)	Density CO ₂ (g/cm ³)	Comp Mole (%)	Salinity (%)	Comments
Theta reef	185 - 325	200	>.85	25-60	9-17	Halite, anhydrite (?)
Blyde reef	max 275 decrepitation domin.	200	.87 - .92	10 - >60		Halite rare
Vaalhoek stockwork	190-200	200	.65 - .93	<5 to 85		No daughters
Trixie leader	>400	175-225	.65 - 80	0 - 30	2-12 plus sylvite	Halite rare
Gregory reef	335-375	300-350	.87 - .95	15 - 35	high, 23	abundant daughters T _h daughters >450° CO ₂ less dominant

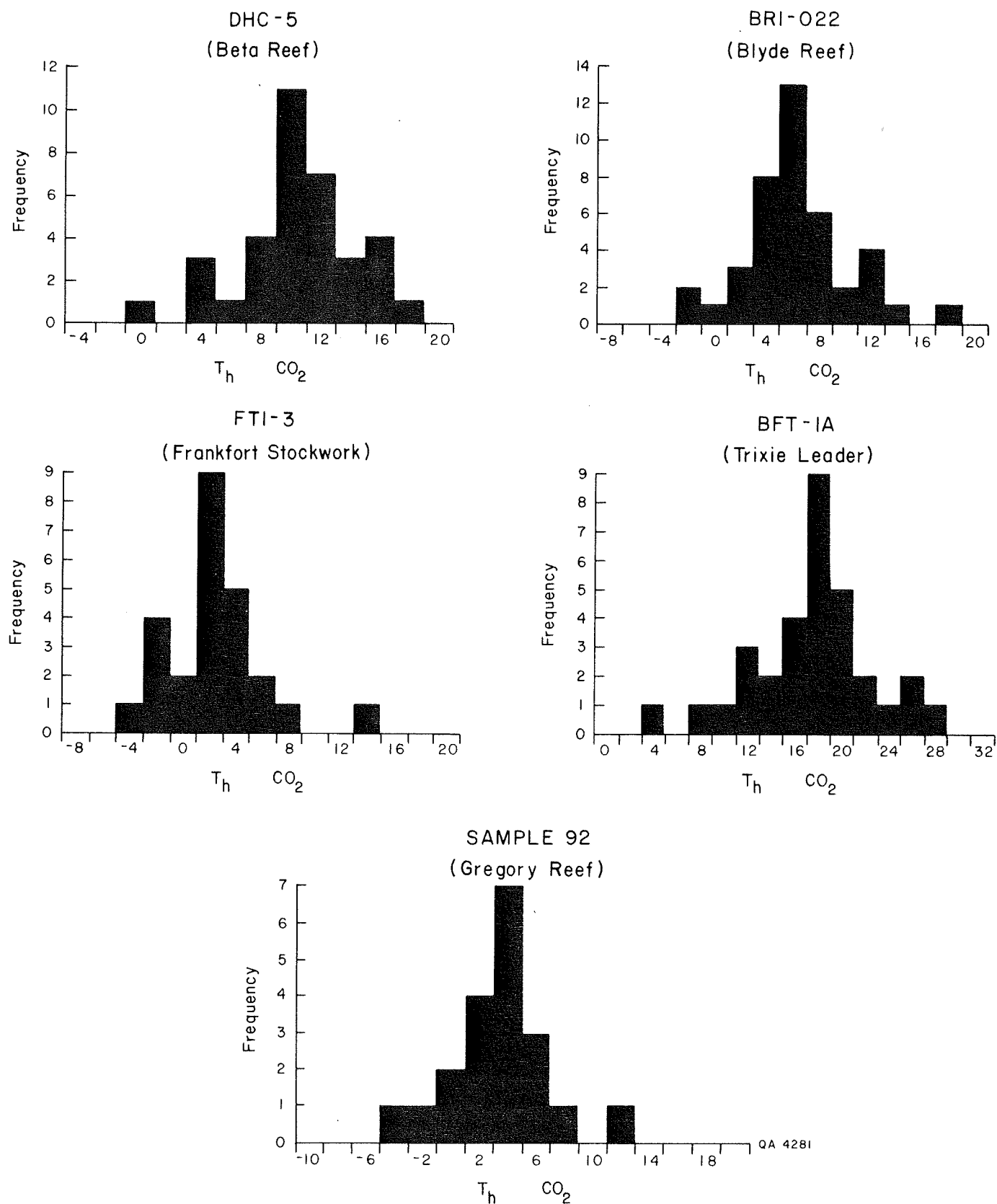
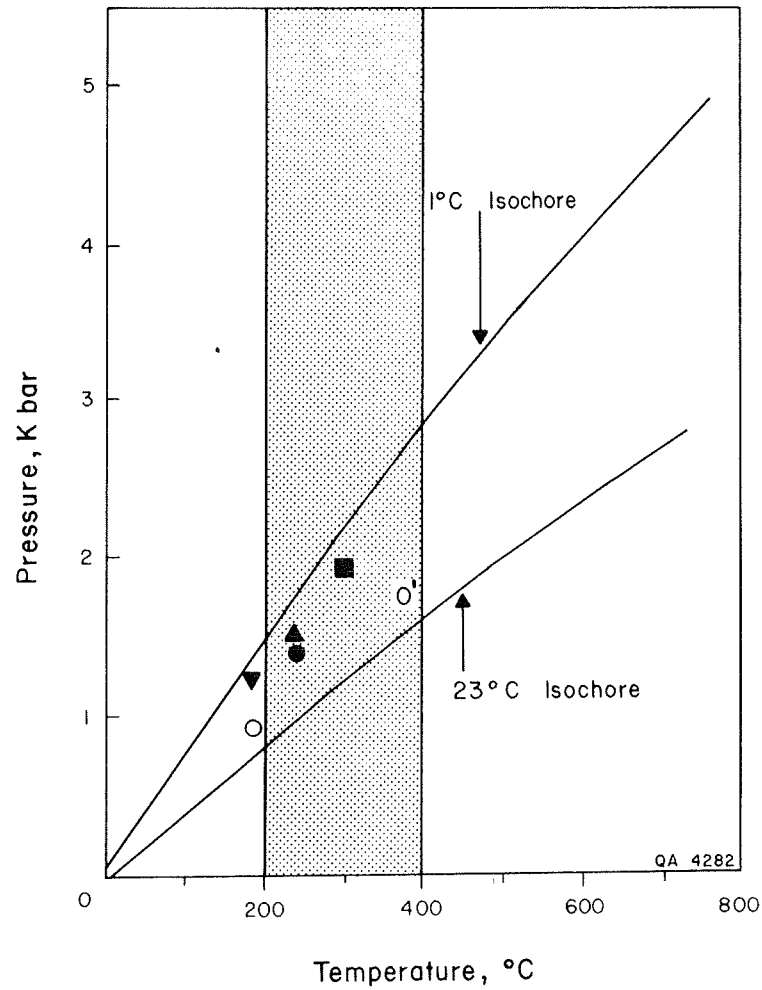


Figure 3 : Histogram-plots of temperature-of-homogenization of CO_2 -rich fluid-inclusions.



HOMOGENIZATION TEMPERATURES

Sample and symbol		Median $T_h(\text{CO}_2)$ °C	Range °C	T_h Median °C	Description
DHC	Theta reef ●	10	200 - 300	240	Stratiform reefs
BRI	Blyde reef ▲	6	200 - 280	240	
FT1-3	Vaalhoek stockwork ▼	3	170 - 210	190	
BFT-1A	Trixie leader ○	18	160 - 270* max >400	190	Stockworks
92	Gregory reef ■	4	270 - 400	300	Vertical reef

*All decrepitation temperatures

Figure 4 : Data-tabulation and P-T- CO_2 isochore plot of Pilgrim's Rest fluid-inclusion data. The shaded area brackets estimated, minimum temperatures-of-formation, as deduced from available, total, homogenization data. Modified from Hollister and Burruss (1976).

This value approaches that of the Gregory Reef, to which it is stratigraphically equivalent. By contrast, the Vaalhoek stockwork displays formation-pressures and -depths of 1,25 kbars and 4,6 km, respectively. This apparent depth-of-formation is inconsistent with pressure/depth data obtained from the other ore-bodies, being too shallow for its stratigraphic setting. Unlike the Trixie Leader, this sample displayed a tight grouping of well-defined homogenization- and decrepitation-temperatures (Fig. 2), suggesting the data to be valid. One possible reason for the abnormally-low pressures-of-formation is the structural setting of the stockwork. The Vaalhoek stockwork is a fracture-fill ore-body that lies in close proximity to a major dyke (the Vaalhoek Dyke), which was clearly intruded under tensional conditions. It is suggested that remobilization of ore may have occurred during dyke-emplacement. The remobilized ores were reprecipitated in fractures, at sub-normal pressures, in an extensional tectonic regime. The tight grouping of homogenization- and decrepitation-temperatures of this sample suggests that the fluid-inclusion geobarometer was reset during remobilization.

It must be re-emphasized that these pressures-of-formation are considered preliminary. The problem of decrepitation in a CO₂-rich system, such as Pilgrim's Rest, results in a thin data-base. However, comparison of calculated depths-of-formation of strata-bound reefs and vertical reefs with the known thicknesses of stratigraphic intervals separating these deposits suggests that the estimated pressures- and depths-of-entrapment are reasonable. Most of the samples display a range of decrepitation- and homogenization-temperatures, suggesting that mineralization was a multiphase, rather than a single, event. Thus, the pressure- and temperature-data represent average conditions of formation.

Estimated salinities of Type-1 inclusions (lacking a visible CO₂-phase) range from 5 to greater than 15 weight-per cent NaCl-equivalent (Fig. 5). Carbon dioxide is probably present, in various amounts, in all of the fluid-inclusions, causing over-estimation of salinity-values by the formation of clathrate compounds (Collins, 1979). In addition, halite daughter-minerals and CO₂-rich phases coexist in Type-3 inclusions, complicating the interpretation of the salinity-data in these inclusions. The presence of cations, such as Ca⁺⁺ and K⁺, as indicated by occasional sylvite and anhydrite daughter-minerals, further complicates the interpretation of the salinity-data. Other cations present will tend to decrease the solubility of halite, which can then be present as a crystal-phase, even though the solution contains less than 26,5 weight-per cent NaCl-equivalent (Roedder, 1984). However, the presence of daughter-minerals indicates that the respective fluids were oversaturated, with respect to these phases, at laboratory conditions. When compared to other deposit-types, the Pilgrim's Rest fluid-inclusions are anomalously saline. No apparent relation between sample-location and salinity was indicated in this study.

Comparison of Pilgrim's Rest fluid-inclusion characteristics with other major, precious-metal-deposit types (Table 2) yields some interesting similarities. Homogenization-temperatures of the Pilgrim's Rest deposits are comparable with lode-gold deposits (200 to 400°C). Both deposit-types formed under lithostatic pressures. Both contain ubiquitous, high-density-CO₂ inclusions. Furthermore, lode-gold and the Pilgrim's Rest fluid-inclusions contain accessory methane. These data suggest the Pilgrim's Rest

**TABLE 2. DIAGNOSTIC FLUID INCLUSION CHARACTERISTICS
OF PRINCIPAL ORE DEPOSIT TYPES**

<u>DEPOSIT TYPE</u>	<u>FLUID COMPOSITION</u>	<u>SALINITY (% NaCl)</u>	<u>T_H(°C)</u>	<u>REMARKS</u>
Pilgrims Rest	CO ₂ , H ₂ O ± CH ₄	Saline(?) 15 wt % Daughters	200-400	CO ₂ -rich; Daughter minerals (KCl, NaCl, CaSO ₄); high density CO ₂
Massive Sulfide	H ₂ O	Dilute: 1-8 wt. %	200-370	No boiling
Mississippi Valley	H ₂ O, hydrocarbons	Saline: >15 wt. %	100-150	No boiling
Porphyry Cu	H ₂ O, CO ₂ (rare)	Saline: up to 75 wt. %	up to 750	Boiling common
Porphyry Mo	H ₂ O, CO ₂ (minor)	Moderate: <15 wt. %	up to 500	CO ₂ phase separation
Epithermal Au-Ag	H ₂ O, CO ₂ (minor)	Dilute: <5 wt. %	<350	Boiling common
Sn-W Skarns	H ₂ O, CO ₂ (minor)	10-45 wt. %	600-650	Local boiling
U-veins	H ₂ O, CO ₂ , hydrocarbons	Dilute: 1-5 wt. %	>400	CO ₂ phase separation
Lode Gold	H ₂ O, CO ₂ , CH ₄ (minor)	Dilute: <5 wt. %	200-400	CO ₂ -rich inclusions ubiquitous; high density CO ₂

- 16 -

(after Colvine et al., 1984)

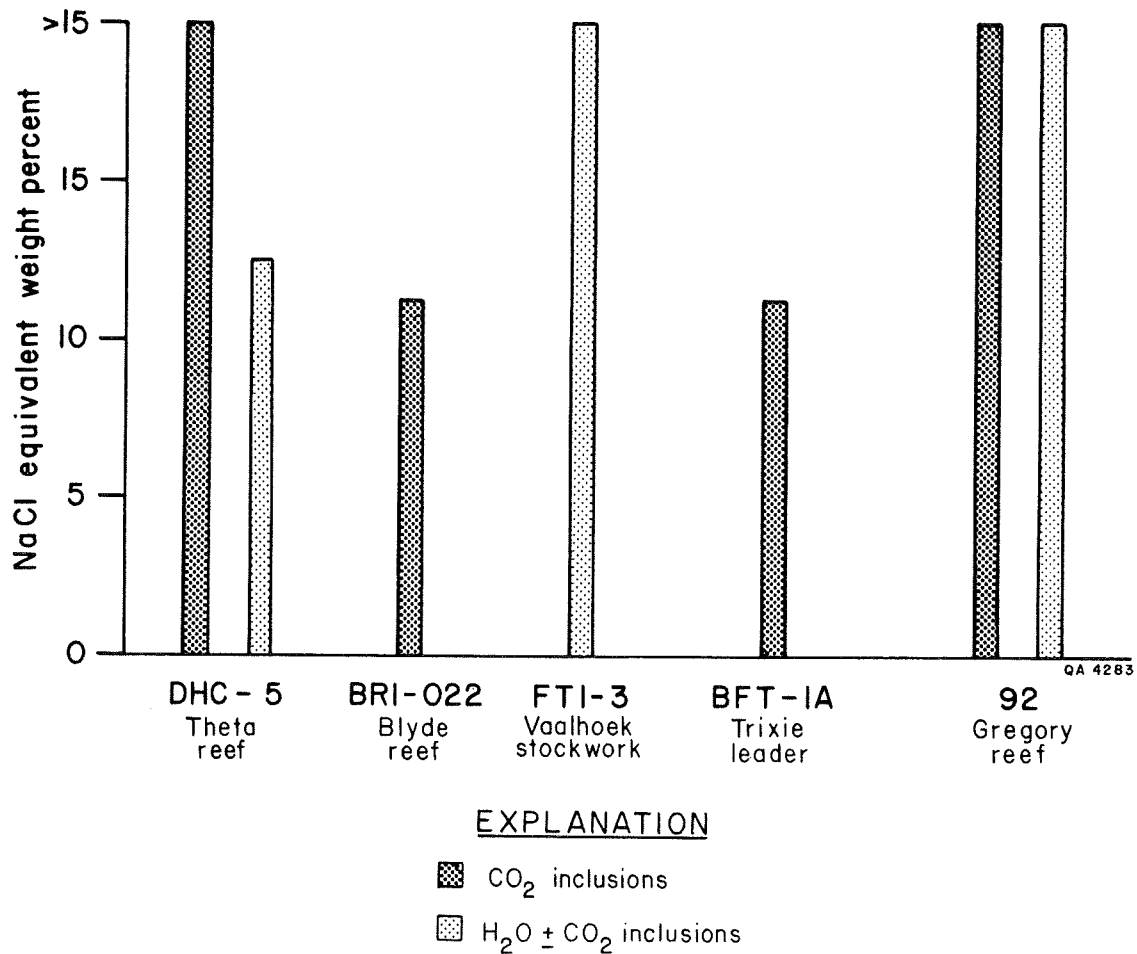


Figure 5 : Salinity-estimates of Pilgrim's Rest fluid-inclusions, based on melting-point-depression measurements of CO₂ and H₂O inclusions.

vein-gold deposits to be comparable with Archean lode-gold deposits and that they may have originated under broadly-similar conditions. A fundamental difference between the two classes of deposits is that lode-gold deposits, as well as epithermal gold deposits (such as Creede, Carlin, and Cortez), were formed from dilute solutions. By contrast, data from Pilgrim's Rest suggest that the mineralizing fluids were moderately-to-highly saline.

CONCLUSIONS

Preliminary investigation of fluid-inclusions from Pilgrim's Rest quartz-vein deposits indicates that the mineralizing fluids were saline and

rich in CO₂. The deeper deposits (e.g. Gregory Reef) contain fluid-inclusions with abundant daughter-elements, suggesting that, at deeper levels, the fluids were high in total dissolved solids. As the shallower deposits contain fewer daughter-minerals, the fluids evolved as they migrated upward, possibly as a response to temperature- and pressure-gradients. The CO₂-content and salinity of the fluid remained consistently high.

Homogenization-temperatures suggest there was a temperature-of-entrapment gradient of at least 100°C over the 1 km of sediment that separates the deeper from shallower ore-bodies. Preliminary geobarometry suggests a pressure-difference of between 400 and 500 bars over the same interval. Pressure-data further suggest that the Pilgrim's Rest precious-metal veins were emplaced at depths of 5,5-7 km. Approximately 8 km of Pretoria-Group sediments and volcanics overlie the Malmani Dolomite in the eastern Transvaal (Button, 1973). It follows that, if the depth-calculations are correct, the veins may have been injected into the basement granites and into the overlying sediment during late-Pretoria time. This was a period of great crustal instability and was marked by the extrusion of up to 1 400 m of basaltic-to-intermediate volcanics known as the Dullstroom Lava. Subsequent differentiation of the magmatic source resulted in the outpouring of an additional 3 000 m of acid lavas (the Rooiberg Felsites). These early-Proterozoic, magmatic events could have been the heat-source that drove the hydrothermal solutions at Pilgrim's Rest. Alternatively, the Bushveld Complex might have provided the requisite, thermal energy; however, in that situation, depths-of-formation would have been closer to 10 and 12 km.

REFERENCES

- Button, A. (1973). A regional study of the stratigraphy and development of the Transvaal Basin in the eastern and northeastern Transvaal. University of the Witwatersrand, Johannesburg, unpub. Ph.D. thesis, 352 p.
- Collins, P. (1979). Gas hydrates in CO₂-bearing fluid inclusions and the use of freezing data for the estimation of salinity. *Econ. Geol.*, 74, 1435-1444.
- Colvine, A., et al. (1984). An integrated model for the origin of Archean lode gold deposits. Ontario Geol. Survey, Open File Rept. 5524, 101 p.
- Hollister, L.S., and Burruss, R.C. (1976). Phase equilibria in fluid inclusions from the Khtada Lake metamorphic complex. *Geochim. Cosmochim. Acta*, 40, 163-175.
- Nash, J.T. (1972). Fluid inclusion studies of some gold deposits in Nevada. U.S. Geol. Survey, Prof. Paper 800-C, C15-C19.
- Roedder, E. (1984). Fluid inclusions. *Reviews in Mineralogy, Mineralogical Soc. Am.*, 12, 644 p.
- Swiegers, J.U. (1948). The gold deposits of the Pilgrim's Rest gold mining district. *Trans., Geol. Soc. S. Afr.*, 51, 82-132.

APPENDIX 1

Microthermometric Results
CO₂-H₂O± NaCl Inclusions

Sample#	Estimated vol.% CO ₂	Melting Temp(°C)			Homogenization Temp(°C)		
		CO ₂	H ₂ O	Hydrate	CO ₂	CO ₂ +H ₂ O	Daughter
DHC-5 Theta reef	35	-57	-10.3	+8.5(?)	+3.5	208.5	
	25	-56.5	-12.2	nd	+3.8	>225	
	30	-57.1	nd	+9.0	+12.6	217.5	297 (H)
	60	nd	nd	nd	+11.1	>220	
	<1	nd	-9.6	nd	nd	238.6	
	45	-56.8	nd	nd	+6.2	>223	
	55	-57.2	nd	nd	+4.5	>214	
	25	-56.9	nd	+8.5(?)	+2.4	195.6	>286 (H)*
	20	nd	-11.5	nd	-1.0	>285	
	35	-56.2	nd	nd	+10.5	238.1	325 (H)*
	45	-56.7	nd	nd	+4.2	>240	
	50	-56.6	nd	nd	+14.8	>220	
	75	-59.1	nd	+12.1(?)	+16.6	>200	
	25	-56.8	-9.7	nd	+6.8	>245	
	50	-56.6	nd	nd	+7.6	>220	
	35	-56.0	-11.2	nd	+9.3	>220	
	<5	nd	-8.8	nd	nd	290.5	
	55	-56.9	nd	nd	+9.8	>220	
	25	-56.6	nd	nd	+15.8	>245	
	45	-57.0	nd	nd	+8.8	>220	
	25	-56.8	nd	nd	+8.0	>195.7	>300 (H)
BR1-022 Blyde reef	80	-57.7	nd	+9.6	+2.2	>205	
	75	-57.1	nd	nd	-2.6	>210	
	40	-56.9	-8.1	nd	+5.1	>210	
	35	-56.6	-9.6	nd	+8.8	>210	
	35	nd	nd	nd	+7.1	225	278 (H)
	90	-56.7	nd	nd	+2.0	>210	
	65	nd	nd	nd	+3.8	>210	
	25	-56.9	-7.9	nd	+13.5	260.7	
	25	-56.8	-11.5	nd	+10.7	>255	
	50	-57.0	nd	nd	+6.7	260(?)	
	50	-56.7	nd	+12.3	+7.7	>235	
	35	-56.8	-10.2	nd	+8.0	>265	
	10	-56.9	nd	nd	+16.6	>275	
	75	-57.8	nd	nd	+2.1	>200	
	35	nd	nd	nd	+5.5	nd	
	50	-56.6	nd	+11(?)	+5.5	>225	

nd = no data (H) = halite daughter mineral
 > = temp. decrepitation * = non-homogenizing daughter phase
 (?) = non-reproducible

APPENDIX 1 (cont.)

Sample#	Estimated vol.% CO ₂	Melting Temp(°C)			Homogenization Temp(°C)		
		CO ₂	H ₂ O	Hydrate	CO ₂	CO ₂ +H ₂ O	Daughter
FT1-3	25	-56.7	-19.6	nd	+6.6	187.5	
Vaalhoek stockwork	10	nd	-20.6	nd	+12.2	195(?)	
	35	-56.9	nd	nd	+3.5	189.8	
	65	-58.1	nd	nd	-2.6	>200	
	65	-57.2	nd	nd	+1.0	193.4	
	30	-56.8	-19.9	+12.8	+5.3	173.8	
	35	nd	-18.3	+11.1(?)	+3.5	208.8	
	85	nd	nd	nd	+4.0	>200	
	75	-58.3	nd	nd	+1.2	>195	
	45	-56.5	nd	nd	+5.5	>195	
	45	nd	-17.1	nd	+1.0	196.7	
	50	-56.7	nd	nd	+1.5	>190	
	75	-56.7	nd	nd	+0.5	>200	
	50	-57.1	nd	nd	-4.6	>175	
	50	-56.5	-18.8	nd	+2.0	201.5	
BFT1-A	20	-56.7	-9.2	nd	+24.6	>175	
Trixie leader	35	-56.6	nd	nd	+8.8	>200	
	10	nd	-4.0	nd	+20.6	>250	
	35	-56.8	nd	nd	+11.6	>250	
	60	-56.9	nd	nd	+14.6	>200	
	75	-57.1	nd	nd	+17.0	>175	
	25	nd	-8.9	nd	+16.5	>180	
	40	nd	nd	nd	+16.9	>210	
	75	-58.0	nd	+13.0(?)	+10.1	>175	
	20	nd	-10.5	nd	+19.4	>245	
	15	nd	nd	nd	nd	>265	
	50	-56.7	nd	nd	+17.5	245(?)	
	75	-58.1	nd	nd	+12.1	>195	
	50	-56.6	nd	nd	+17.1	>195	
	50	-57.7	nd	nd	+6.5	>200	
	95	-58.5	nd	+12.2	+3.8	>225	
	30	-56.8	-11.6	nd	+20.6	>160	
	40	-56.6	nd	nd	+19.0	>180	
	60	-57.2	nd	nd	+22.8	>175	
	85	-57.9	nd	nd	+10.8	>175	
	75	-58.6	nd	nd	+24.8	>200	
	35	-56.9	-13.9	+7.2(?)	+6.7	>240	
	75	-60.2	nd	nd	+26.9	>185	

nd = no data
 > = temp. decrepitation
 (?) = non-reproducible
 (H) = halite daughter mineral
 * = non-homogenizing daughter phase

APPENDIX 1 (Cont.)

Sample#	Estimated vol.% CO ₂	Melting Temp(°C)			Homogenization Temp(°C)		
		CO ₂	H ₂ O	Hydrate	CO ₂	CO ₂ +H ₂ O	Daughter
92 Gregory reef	10	nd	-22.4	nd	-2.8	115.8	228.6 (H) *
	20	-56.5	nd	nd	+1.1	>325	
	35	-56.7	-19.1	nd	+4.1	>325	
	75	-57.9	nd	nd	+11.0	>300	
	5	nd	nd	nd	nd	395	
	10	nd	nd	nd	nd	305	>425.0 (H) *
	25	-56.8	-21.5	nd	+4.8	>300	
	50	-57.5	nd	+8.8(?)	+3.5	>300	
	45	-56.1	nd	nd	-0.5	>285	
	35	-56.7	nd	nd	+3.5	375	
	50	-58.0	nd	+13.6(?)	+3.2	>325	
	25	-57.1(?)	nd	nd	+6.8	125.0	>395 (H)
	30	nd	-19.2	nd	nd	>300	>300 (H)
	50	-56.9	nd	nd	+3.5	>350	
	50	-57.3	nd	nd	+4.9	>350	
	60	-57.1	-18.6	nd	+1.9	>325	
	30	-56.6	-20.1	nd	+5.2	>350	
	40	-56.7	nd	nd	+3.9	>355	
	50	-56.8	nd	nd	+3.7	>365	
	75	-57.7	nd	nd	+2.8	>275	

nd = no data
 > = temp. decrepitation
 (?) = non-reproducible
 (H) = halite daughter mineral
 * = non-homogenizing daughter phase